BIOCHEMISTRY
including biophysical chemistry & molecular biology

Article

pubs.acs.org/biochemistry

Structure–Function Mapping of Key Determinants for Hydrocarbon Biosynthesis by Squalene and Squalene Synthase-like Enzymes from the Green Alga *Botryococcus braunii* Race B

Stephen A. Bell,[†,‡] Thomas D. Niehaus,[†,§] S. Eric Nybo,[†,‡,∥] and Joseph Chappell*[,†,‡]

[†]Plant and Soil Sciences, University of Kentucky, Lexington, Kentucky 40546-0312, United States

[‡]Pharmaceutical Sciences, University of Kentucky, Lexington, Kentucky 40536-0596, United States

Supporting Information

ABSTRACT: Squalene and botryococcene are branched-chain, triterpene compounds that arise from the head-to-head condensation of two molecules of farnesyl diphosphate to yield 1′−1 and 1′−3 linkages, respectively. The enzymes that catalyze their formation have attracted considerable interest from the medical field as potential drug targets and the renewable energy sector for metabolic engineering efforts. Recently, the enzymes responsible for botryococcene and squalene biosynthesis in the green alga *Botryococcus braunii* race B were characterized. To better understand how the specificity for the 1′−1 and 1′−3 linkages was controlled, we attempted to identify the functional residues and/or domains responsible for this step in the catalytic cascade. Existing crystal structures for the mammalian squalene synthase and *Staphylococcus* dehydrosqualene synthase enzymes were exploited to develop molecular models for the *B. braunii* botryococcene and squalene synthase enzymes. Residues within the active sites that could mediate catalytic specificity were identified, and reciprocal mutants were created in an attempt to interconvert the reaction product specificity of the enzymes. We report here the identification of several amino acid positions contributing to the rearrangement of the cyclopropyl intermediate to squalene, but these same positions do not appear to be sufficient to account for the cyclopropyl rearrangement to give botryococcene.

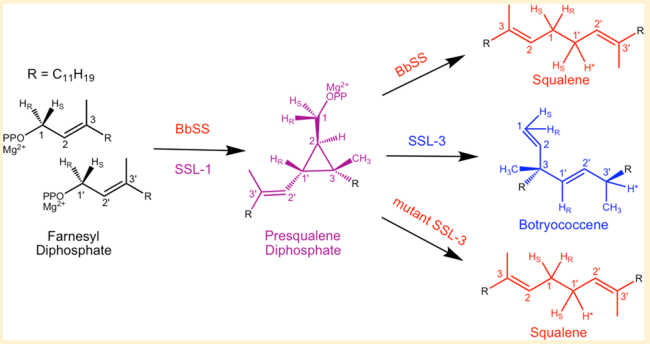

Squalene is a linear, branched-chain hydrocarbon composed of six isoprene units. It is the first committed intermediate for sterol biosynthesis in eukaryotes and hopanoid biosynthesis in prokaryotes, end products that play essential roles in a variety of cellular functions and contribute to the physical properties of membranes.[1,2] Squalene synthase catalyzes the biosynthesis of squalene via two reaction steps using a reaction mechanism common to all eukaryotic squalene synthases.[3−6] Briefly, two molecules of farnesyl diphosphate (FPP) are joined together in a head-to-head coupling to yield the stable, cyclopropyl intermediate presqualene diphosphate (PSPP) in the first reaction step, which is NADPH-independent (Scheme 1).[7,8] PSPP remains in the active site where, in the presence of NADPH, it is reductively rearranged to give the final 1′−1 linked, symmetrical squalene molecule in the second reaction step.[3,9,10] Normally, squalene is the sole product observed when squalene synthase is incubated with NADPH and FPP. However, in the absence of NADPH and upon prolonged incubation, squalene synthase is known to generate various 1′−1 and 1′−3 linked solvolytic products, along with the cyclopropyl intermediate.[10,11]

Kinetic analyses performed with *Saccharomyces cerevisiae* squalene synthase (ScSS)[3,5,9,10] and detailed crystallographic studies of *Homo sapiens* squalene synthase (HsSS)[6,12,13] and *Staphylococcus aureus* dehydrosqualene synthase (CrtM)[14] have provided insight into how the two molecules of FPP bind in these enzymes and subsequently rearrange to yield squalene or dehydrosqualene. However, fewer studies have been conducted to elucidate specific roles that active site residues play in the complicated catalytic cascades of these enzymes. On the basis of simple amino acid sequence alignments, Robinson et al. predicted that the five highly conserved domains among squalene synthases were likely helices that lined the active site pocket.[15] This prediction has since been confirmed by structural evidence.[6,12,13] Other studies have utilized site-directed mutagenesis to confirm roles for several residues among the conserved domains as well as loop regions.[4,12,16] Gu et al., for example, showed that the Asp-rich (DXXED) motifs serve to coordinate divalent cations, which in turn facilitate binding of the diphosphate substituents of FPP at the entrance to the hydrophobic active site pocket and possibly contribute to the initiating ionization event.[4] Liu et al. and Furubayashi et al. have since provided evidence of a novel NADPH binding site

Received: October 7, 2014
Revised: November 12, 2014
Published: November 13, 2014

   dx.doi.org/10.1021/bi501264s | *Biochemistry* 2014, 53, 7570−7581

Scheme 1. Proposed Catalytic Cascades for the Enzyme-Mediated Biosynthesis of Squalene and Botryococcene[a]

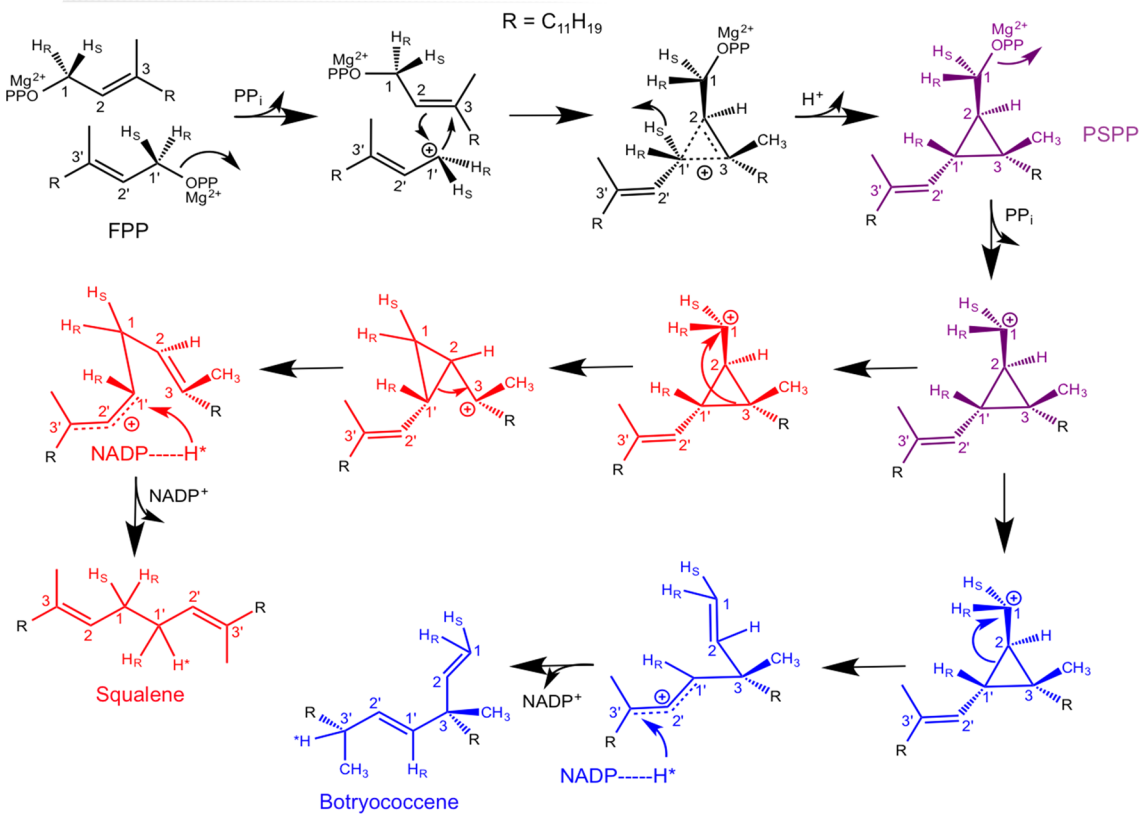

[a]Adapted from refs 40 and 20.

by demonstrating that specific mutations within the conserved domains and an additional conserved region (J/K loop) result in squalene synthases that yield dehydrosqualene rather than the reduced form of squalene.[12,16] However, this effect could be overcome when the mutant enzymes were incubated with an excess of NADPH.[12]

Defined roles for the highly conserved domains with respect to their involvement in substrate orientation and product specificity have not yet been described empirically. Detailed maps of the residue(s) important for the first or second reaction step or both that correlate with kinetic and structural data have also not been functionally identified. Hence, the current effort set out to exploit some unique, newly characterized triterpene synthases with the aim of interconverting catalytic specificities to finely map structure−function relationships.

Botryococcene, an analogue of squalene, is produced by the green alga *Botryococcus braunii* race B in copious amounts.[17,18] Because of structural similarities between botryococcene and squalene, botryococcene was predicted to arise via a squalene synthase-like reaction that proceeds through PSPP like squalene biosynthesis.[19] However, instead of the reductive rearrangement to the 1′−1 linkage found in squalene, a rearrangement to a more branched 1′−3 molecule was proposed (Scheme 1).[19−21] Interestingly, Niehaus et al. recently identified the enzymes responsible for botryococcene biosynthesis and found two distinct squalene synthase-like enzymes, SSL-1 and SSL-3, were necessary.[22] This came in opposition to the original assumption that a single squalene synthase-like enzyme would catalyze both reaction steps.[21−23] SSL-1 was shown to efficiently catalyze the biosynthesis of PSPP from FPP, while SSL-3, which could not utilize FPP as a substrate, was readily able to convert PSPP to botryococcene in a reductive rearrangement that required NADPH.[22]

The discovery of distinct SSL enzymes presented a unique opportunity to aid in the identification of particular amino acid residues contributing to the specificity of the first and second reaction step activities in squalene and botryococcene biosynthesis. Hence, we hypothesized that it might be possible to use rational, site-directed mutagenesis either to introduce a missing reaction step into one of the respective SSL enzymes (i.e., introduce botryococcene second-step reaction capability into SSL-1 to create a single enzyme capable of catalyzing the conversion of FPP to botryococcene) or to convert SSL-3 product specificity from botryococcene to squalene.

MATERIALS AND METHODS

Three-Dimensional (3D) Modeling. Generation of 3D models for the *B. braunii* triterpene synthases was accomplished using MODELLER 9v8.[24] Online tutorials for basic modeling were followed using empirically determined structures of HsSS [Protein Data Bank (PDB) entries 1EZF and 3VJ8][6,13] and CrtM (PDB entry 2ZCO)[14] as templates. *B. braunii* GenBank accession numbers are as follows: BbSS, AF205791.1; SSL-1, HQ585058.1; and SSL-3, HQ585060.1. Models were generated by first performing an alignment of the template and *B. braunii* enzyme of interest using MODELLER 9v8. The *B. braunii* enzyme sequence was then trimmed at its amino- and carboxy-terminal ends to match the length of the template. A second alignment was performed with the truncated *B. braunii* sequence and original template; this alignment was then used for the modeling program. All parameters were left as default

dx.doi.org/10.1021/bi501264s | *Biochemistry* 2014, 53, 7570−7581

with five models generated for each run. Models with the lowest DOPE score were chosen for subsequent analyses.

Substrate Docking. PSPP was docked into HsSS (PDB entry 3VJ8) and the *B. braunii* 3D models of BbSS and SSL-3 that were threaded onto 3VJ8 using the Genetic Optimisation for Ligand Docking program (GOLD; Cambridge Crystallographic Data Centre, Cambridge, U.K.).[25] Proteins were set up as follows: all hydrogens were added, all waters and ligands removed, and distance constraints (3.5−4.5 Å) set to anchor the C11 prenyl chain to L184, the C9 prenyl chain to Y280, and the cyclopropyl methyl to L212 [distance constraints based on measurements of CrtM-PSPP (PDB entry 3ADZ)]. The conserved residues listed are numbered according to BbSS. The binding site was defined as a sphere with a 10 Å radius centered on V180 in domain II. Twenty-five runs were performed for each GOLD run with 1 million operations per run. Hydrophobic constraints were put on all hydrophobic residues within the active site sphere and all hydrophobic ligand atoms during docking runs. The PSPP file used for docking was created using atom coordinates from PSPP cocrystallized with CrtM (PDB entry 3ADZ).[14] These coordinates were submitted to the PRODRG server[26] (University of Dundee, Dundee, U.K.) with the "chirality", "EM", and "charges" options selected as yes, reduced, and yes, respectively. The MDL Molfile output with all hydrogens was saved in mol2 file format and used for docking. All other parameters were left as default during docking runs.

Wild-Type *B. bruanii* Triterpene Synthase Cloning. Primers used to construct genes described in this section can be found in Table S2 of the Supporting Information; plasmid DNA (courtesy of T. D. Niehaus)[22] was used as template. All wild-type and mutant genes used in this study were directionally cloned into the pET28a vector (Novagen) *Nde*I and *Hin*dIII sites such that expressed enzymes would contain an amino-terminal hexahistidine tag that could be used for purification and immunodetection. SSL-3 had an internal *Hin*dIII site intentionally altered at the time it was cloned into pET28a; mutants subsequently constructed from it contained the *Hin*dIII site deletion. Because BbSS and SSL-2 were predicted to be membrane-bound enzymes,[22,27] they were truncated at their carboxy-terminal ends 65 and 87 amino acids, respectively, to produce catalytically competent, soluble enzymes that could be expressed in *Escherichia coli*. For *in vivo* analyses of mutants co-expressed with SSL-1 or SSL-3 in *E. coli*, SSL-1 and SSL-3 were cloned into MCS1 *Nco*I and *Hin*dIII sites of pACYCDuet-1 (Novagen). All constructs were verified by BigDye Terminator automated sequencing (ABI).

Polymerase Chain Reaction (PCR) Construction of Mutant Genes. Sequence overlap extension polymerase chain reaction (SOE PCR)[28] afforded the ability to construct mutants described in this work as follows. Internal primers containing the altered nucleotide(s) of interest (IF and IR primers in Table S2 of the Supporting Information) were used along with either the 5′ or 3′ end primer to amplify the gene of interest in two fragments in two separate reactions. The two gene fragments were gel purified and used as templates in a second SOE PCR with the 5′ and 3′ end primers to reassemble the mutated gene. The reassembled gene was gel purified, digested with *Nco*I and *Hin*dIII, and ligated into *Nco*I and *Hin*dIII doubly digested pET28a. Reassembly was routinely performed with up to four fragments of a gene in an SOE PCR. Conditions for the first PCR and second SOE PCR were as follows: 98 °C, 1 min initial denaturation followed by 25 cycles of 98 °C, 10 s to reach 55 °C, and 15 s to reach 72 °C, 1 min/kb with a final elongation step of 72 °C for 10 min. All constructs were verified by BigDye Terminator automated sequencing (ABI).

Construction of a Methyl Erythritol Phosphate (MEP) Pathway Overexpression Cassette. pSB1:operon3 plasmid construction involved relocating the tetracycline resistance (Tet^R) marker from pBBR1MCS-3 to the pBBR1MCS-2 backbone.[29] To accomplish this, the kanamycin resistance (Kan^R) marker was removed by first digesting pBBR1MCS-2 with *Bgl*II and then treating with Klenow to obtain blunt ends. This product was then digested with *Kpn*I to excise the Kan^R gene from the vector completely followed by gel purification of the vector backbone. Tet^R was then digested from pBBR1MCS-3 with *Kpn*I and *Zra*I and ligated into the pBBR1MCS-2 backbone; clones containing the Tet^R marker were isolated via tetracycline resistance selection on LB-Tet plates (12.5 mg/L). This vector was named pSB. The A1/03/04 Lac promoter was amplified by PCR from pIND4 (courtesy of J. Armitage)[30] using the 5′ *Sac*I plac and 3′ *Xba*I plac primers and cloned into the *Sac*I and *Xba*I sites of pSB, resulting in expression vector pSB1. To enhance *in vivo* titers of the substrate FPP, a synthetic operon consisting of a deoxyxylulose 5-phosphate synthase gene (DXS) and the isopentenyl diphosphate isomerase gene (IDI) from *E. coli* and a farnesyl diphosphate synthase gene (FPS) from *Gallus gallus* (chicken) was constructed. The genes were synthesized (GenScript Corp.) as a single polycistron with an optimized Shine Dalgarno sequence (AGGAGGA) in front of each gene for expression in *E. coli*.[31] The operon consisting of DXS, IDI, and FPS was digested from pUC57-operon3 as an *Xba*I and *Bam*HI fragment and subcloned into the same sites of pUC19 to give construct pUC19:operon3. The entire operon3 was then subcloned into pSB1 as an *Xba*I and *Kpn*I fragment to afford pSB1:operon3. This construct was functionally verified in *E. coli* BL21(DE3) by co-expressing it with pET28a:BbSS and analyzing squalene levels. Additionally, each gene of operon3 was individually cloned into pSB1 using the *Xba*I and *Kpn*I sites in pSB1 to yield vectors pSB1:DXS, pSB1:IDI, and pSB1:FPS. These constructs were verified by BigDye Terminator automated sequencing (ABI).

Protein Expression. The following general scheme for protein expression was utilized throughout the course of this work for all wild-type and mutant enzymes assessed. Fresh transformations of *E. coli* BL21(DE3) (Life Technologies) cells with a given construct were always performed. Single colonies were selected to start 2 mL LB-Kan (50 mg/L) cultures that were incubated overnight at 37 °C on a platform shaker; 500 μL of the overnight culture was used to inoculate 50 mL of Terrific Broth (TB) supplemented with 1% glycerol and 50 mg/L Kan in a 250 mL flask. Cultures were incubated at 37 °C for 2 h on a platform shaker, cooled on ice for 2−3 min, and induced with isopropyl β-D-1-thiogalactopyranoside (IPTG) (final concentration of 0.5 mM). Protein expression was allowed for 5 h at 23 °C on a platform shaker. Cultures were divided into 10 mL aliquots and centrifuged (2000*g* for 10 min) to pellet cells; growth medium was decanted, and pellets were stored at −80 °C for use up to 2 weeks later.

Hot [^{3}H]FPP *in Vitro* Enzyme Assays. Activity screening assays were conducted as described by Niehaus et al. and Okada et al.[22,23] General assays were performed as follows. Cell culture pellets (10 mL) were thawed on ice and reconstituted in 1 mL of cold reaction buffer [50 mM MOPS (pH 7.3), 2.5 mM β-mercaptoethanol, and 20 mM $MgCl_2$]. Cells were lysed

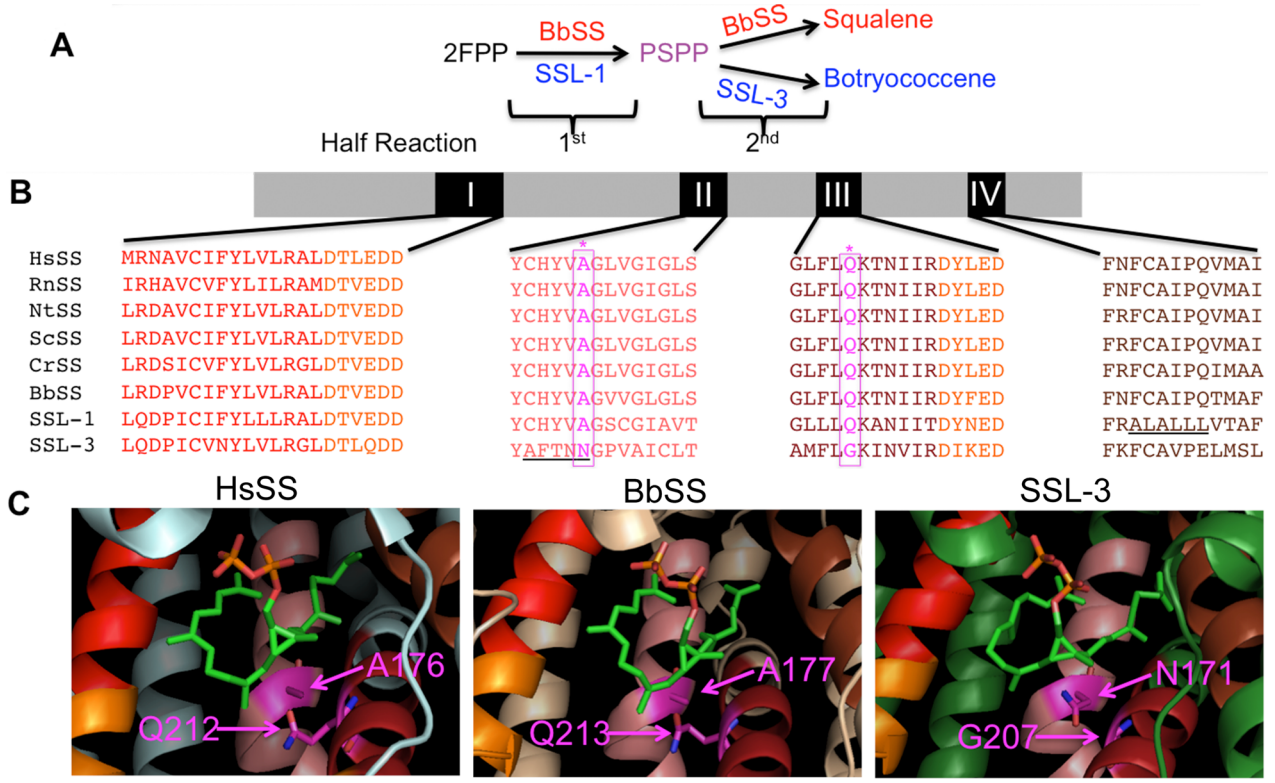

Figure 1. Strategy for identification of residues important for first- and second-reaction step activities and product specificity in triterpene synthases. (A) Simplified biosynthetic pathway for squalene and botryococcene depicting the first and second reaction steps and the enzymes responsible for them. FPP represents farnesyl diphosphate and PSPP presqualene diphosphate. (B) Map of the domain organization of a general triterpene synthase (without the carboxy-terminal membrane-spanning region) and protein sequence alignment of conserved domains I–IV from *H. sapiens* squalene synthase (HsSS), *Rattus norvegicus* squalene synthase (RnSS), *Nicotiana tabacum* squalene synthase (NtSS), *S. cerevisiae* squalene synthase (ScSS), and *Chlamydomonas reinhardtii* squalene synthase (CrSS) as well as the *B. braunii* (Bb) suite of triterpene synthases. Underlined residues denote regions of SSL-3 and SSL-1 significantly different from those of BbSS hypothesized to contribute to their lack of first- and second-reaction step activities, respectively. (C) Crystal structure of HsSS (PDB entry 3VJ8) and 3D models of BbSS and SSL-3 with PSPP (green and orange stick figure) docked into them. Residues labeled in pink represent positions interchanged between BbSS and SSL-3 that were tested for their contribution to reaction product specificities in BbSS and SSL-3.

using a probe dismembranator (50% power, three bursts, 10 s each, 5 min ice between bursts) at 4 °C followed by centrifugation clarification (4 °C, 10000*g*, 10 min). Five microliters of crude lysate(s) was used in 50 μL assays with 30 μM FPP (specific activity of ≈1250 DPM/pmol) and 5 mM NADPH. The reaction mixture was incubated at 37 °C for 30 min followed by termination with 50 μL of 2× stop reagent (0.4 M NaOH and 0.2 M EDTA). Hydrocarbon products were extracted with 200 μL of hexane; 150 μL of organic phase was transferred to a fresh tube, dried to completion, and resuspended in 15 μL of hexane. All 15 μL of resuspended products was used for TLC (silica gel 60 plates, hexane solvent) to separate botryococcene and squalene. Authentic standards of squalene and botryococcene were run alongside experimental samples to define zones from which the silica gel was scraped into a scintillation vial, dissolved in 4 mL of scintillation cocktail, and quantified using scintillation spectroscopy.

Cold FPP *in Vitro* Enzyme Assays. Assays containing only one enzyme were incubated with 50 μM FPP in a volume of 400 μL for 30 min at which point 100 μL of 25 mM NADPH was added or 100 μL of reaction buffer for assays without NADPH. The reaction mixture was then incubated at 37 °C for an additional 30 min until 500 μL of stop reagent was added. Coupled assays performed with two enzymes were conducted identically as just described except that 50 μL of BbSS, M3–11, SSL-3, or M4–10 crude lysate was added in addition to NADPH (50 μL of a 50 mM solution) or buffer (50 μL) after the first 30 min incubation at 37 °C. Hydrocarbon product analysis consisted of two 1 mL extractions with hexane in which 900 μL of the organic phase was transferred to a fresh vial and dried to completion after each extraction. Samples were reconstituted in 50 μL of hexane followed by gas chromatography–mass spectrometry (GC–MS) analysis of 1 μL. GC–MS analyses were performed on an Agilent 7890A gas chromatograph equipped with an HP-5MS column (30 m × 0.25 mm × 0.25 μm) coupled to an Agilent 5975C insert XL MSD instrument with a Triple-Axis Detector (Agilent Technologies, Inc.). The initial oven temperature was held at 150 °C for 1 min followed by two ramps: 10 °C/min to 280 °C and then 5 °C/min to 310 °C and held for 1 min. The mass spectral scan range was from 50 to 500 amu.

Radiolabeled Crude Relative Efficiency Assays. Reaction schemes were based on the work of Greenhagen et al. in which product accumulation was measured using incremental amounts of one enzyme and a constant amount of another enzyme in a coupled assay as an assessment of enzyme efficiency.[32] Crude lysates for these assays were prepared identically as described above. Total protein amounts in crude lysates were measured using a Bradford dye assay and quantified using a BSA standard curve. Scheme A assays were

dx.doi.org/10.1021/bi501264s | *Biochemistry* 2014, 53, 7570–7581

set up with increasing amounts (0, 1, 2.5, 5, and 7.5 μg) of SSL-1 crude lysate in a 40 μL reaction mixture with 50 μM FPP (specific activity of ≈250 dpm/pmol) under the same reaction buffer conditions described above. Reaction mixtures were incubated at 37 °C for 30 min, at which point 5 μL of 50 mM NADPH was added followed by 5 μg of SSL-3 or M4−10. Reaction final volumes were adjusted to 50 μL with reaction buffer and incubated at 37 °C for an additional 30 min followed by termination, extraction, and analysis as described above. Scheme B assays were set up with a constant amount (2.5 μg) of SSL-1 in a 40 μL reaction mixture with 50 μM FPP (specific activity of ≈250 dpm/pmol). Reaction mixtures were incubated at 37 °C for 30 min until 5 μL of 50 mM NADPH was added followed by the addition of increasing amounts (0, 1, 2.5, 5, and 7.5 μg) of either SSL-3, M4−10, BbSS, or M3−11 crude lysates. Final volumes were adjusted to 50 μL with reaction buffer and incubated at 37 °C for an additional 30 min. The calculation of relative efficiency was made as follows: picomoles of squalene per assay for M4−10 with 1 μg of SSL-1 divided by picomoles of botryococcene per assay for SSL-3 with 1 μg of SSL-1; this value was then multiplied by 100. For example, (43.09/53.98) × 100 = 79.82%. Percentage values for the other amounts of SSL-1 tested were then calculated; all percentage values were then averaged to yield the final relative efficiency for the given scheme (A or B) (mutant activity/wild-type activity × 100 for each varying amount and then averaged to yield the final relative efficiency)

***In Vivo* Chemical Profiling.** Wild-type and mutant triterpene synthases were chemically profiled *in vivo* by co-expressing operon3, a triterpene synthase, and the pACYC-Duet-1 expression vector containing SSL-1 or SSL-3 (for triterpene synthase only analyses, the empty pACYCDuet-1 vector was made to account for the metabolic burden of maintaining the additional plasmid in co-expression analyses). Initially, pSB1:operon3 was transformed into *E. coli* BL21-(DE3) cells and plated on LB-Tet (12.5 mg/L); from this transformation, a single colony was selected to generate competent cells. Competent cells were then transformed with a pET28a construct and pACYCDuet-1 construct or empty pACYCDuet-1. Transformations were plated on LB-Tet-Kan-Chlr (12.5 mg/L Tet, 25 mg/L Kan, and 12.5 mg/L Chlr). Single colonies were chosen and cultured in 2 mL of LB-Tet-Kan-Chlr overnight at 37 °C on a platform shaker; 50 μL of an overnight culture was used to inoculate 5 mL of TB-Tet-Kan-Chlr, which was grown at 37 °C for 2 h on a platform shaker. Cultures were then cooled on ice for 2−3 min until IPTG was added (final concentration of 0.5 mM) followed by incubation at 23 °C for 24 h on a platform shaker. Samples were frozen at −80 °C until they were needed. Extractions were conducted in 4 mL screw cap vials using 1 mL of culture, 1 mL of acetone, and 1 mL of hexane. Extraction mixtures were vortexed vigorously five times for 30 s before centrifugation at 2000*g* for 2 min; 350 μL of the organic phase was transferred to a 2 mL GC vial insert where it was allowed to evaporate at room temperature. Samples were reconstituted in 50 μL of hexane followed by GC−FID analysis of 1 μL. The oven program used was identical to that described above for GC−MS analyses.

RESULTS

Mutagenesis Strategy. Amino acid positions chosen for mutagenesis were based on three criteria. First, candidate residues needed to be within the conserved domains of squalene synthases. Second, they needed to exhibit differences between squalene synthases and the SSL enzymes. Third, they needed to be positioned such that the amino acid R groups could possibly interact with the substrate or shape the contour of the active site. The first and second criteria were assessed using ClustalW sequence alignments of squalene synthases from various kingdoms and the *B. braunii* triterpene synthases (Figure 1B). The third criterion was analyzed using 3D models that were generated with MODELLER 9v8 and GOLD (Figure 1C).[24] Originally, the *B. braunii* triterpene synthases were threaded onto the HsSS structure (PDB entry 1EZF), which was determined at a resolution of 2.15 Å.[6] Additional molecular models were prepared as higher-resolution structures became available, such as HsSS (PDB entry 3VJ8) and those for CrtM (PDB entries 3ADZ and 2ZCO).[13,14] No significant differences were observed between any of these models. This method led to the identification of 14 specific positions in SSL-1 and 20 in SSL-3 that lacked conservation with squalene synthases from the plant, animal, and fungal kingdoms. Five of these in SSL-1 and 10 in SSL-3 appeared to be capable of interacting with the substrate and/or altering the surface contour of the active site such that the configuration or orientation of reaction intermediates might be influenced (Table S1 of the Supporting Information).

Initial mutants (M1 series) were based on differences in domain II of BbSS and SSL-3 and constructed in domain II of the BbSS backbone to assess the effect on product specificity (Figure 1B). Subsequent mutant series M3 and M4 were rationalized and constructed using the same technique described above in concert with the results from prior *in vitro* activity screens. Table 1 lists the M1, M3, and M4 mutant series with the corresponding mutations and the enzyme backbone into which the mutations were introduced. Two other mutant series pertinent to the current effort were also constructed to assess the importance of a highly conserved tyrosine residue in domain II (M8 series) and the Asp-rich domains present in domains I and III (M11 series). Table 2 lists the M8 and M11 mutant series with the corresponding mutations and the enzyme backbone into which the mutations were introduced.

Table 1. Identification of the Amino Acids Targeted in the M1, M3, and M4 Mutation Series[a]

mutant name	backbone	mutation
M1−4	BbSS	CHYVA → AFTNN
M1−5	BbSS	V176N
M1−6	BbSS	A177N
M1−7	BbSS	V176N/A177N
M3−7	BbSS	Q213G
M3−8	BbSS	Q213N
M3−11	BbSS	A177N/Q213G
M4−3	SSL-3	N171A
M4−4	SSL-3	G207Q
M4−10	SSL-3	N171A/G207Q

[a]The amino acids and their positions within specific triterpene synthases (backbone) and the specific amino acid substitutions are noted.

***In Vitro* Activity Screens for Mutant Triterpene Synthases.** Because the triterpene synthases targeted in this study were mono- or bifunctional enzymes that could catalyze one or both reaction steps, FPP to PSPP, PSPP to triterpene hydrocarbon, or FPP to squalene, an assay capable of measuring each activity was needed. This posed technical

Table 2. Identification of the Amino Acids Targeted in the M8 and M11 Mutation Series[a]

M8 Series Mutants		
mutant name	backbone	mutation
M8−1	BbSS	Y172F
M8−2	BbSS	Y172A
M8−3	SSL-1	Y175F
M8−4	SSL-1	Y175A
M8−5	SSL-2	Y168F
M8−6	SSL-2	Y168A
M8−7	SSL-3	Y166F
M8−8	SSL-3	Y166A
M11 Series Mutants		
mutant name	backbone	mutation
M11−1	BbSS	R76A
M11−2	BbSS	D79A
M11−3	BbSS	E82A
M11−4	BbSS	D83A
M11−5	BbSS	R219A
M11−6	BbSS	D220A
M11−7	BbSS	E223A
M11−8	BbSS	D224A

[a]The amino acids and their positions within specific triterpene synthases (backbone) and the specific amino acid substitutions are noted.

difficulties because PSPP is not available from commercial vendors and its detection in enzyme assays does not lend itself to rapid or high-throughput assays. Hence, assay conditions were designed to provide a facile means for detecting mutant enzymes capable of converting FPP to triterpene hydrocarbon, FPP to PSPP, or PSPP to triterpene hydrocarbon (Figure S1 of the Supporting Information). The assay devised to test bifunctional enzymes was comprised of incubation of the respective enzyme with radiolabeled FPP and measurement of its incorporation into radiolabeled squalene or botryococcene. To measure activity of either the first or second reaction step, mutant enzymes were co-incubated with substrate and either SSL-1 or SSL-3. Because SSL-1 catalyzes only the conversion of FPP to PSPP, this co-incubation tested for a mutant enzyme's ability to utilize PSPP as a substrate for the biosynthesis of squalene or botryococcene. Because SSL-3 catalyzes only the conversion of PSPP to botryococcene, co-incubations with SSL-3 and the mutant enzyme were a measure of the mutant enzyme's ability to catalyze the first reaction step, FPP to PSPP. Because purification of the mutant enzymes from bacterial lysates resulted in variable losses of catalytic activity, bacterial crude lysates were used as a source of enzyme for assays. The levels of enzymes in the bacterial lysates were comparable to one another as determined by immunodetection blotting (Figure S2 of the Supporting Information).

***In Vitro* Analysis of Mutants.** The M1 mutant series was constructed in the BbSS backbone with the intention of interconverting product specificity from squalene to botryococcene. The M1−4 mutant, which encompassed substitution of five adjacent amino acids within domain II of BbSS with those from the corresponding positions in SSL-3, resulted in an inactive mutant, capable of neither the first nor the second reaction step (Figure 2). In contrast, focus on the asparagine cluster within domain II of SSL-3 and the corresponding positions in BbSS proved to be more informative. The M1−7 mutant substituted the native valine at position 176 and alanine at position 177 in BbSS with asparagines. Interestingly, the M1−7 mutant lost the ability to utilize FPP as a substrate. However, upon co-incubation with SSL-1 (a source of PSPP), the yield of squalene was approximately 50% of that of the wild-type enzyme. When the individual mutants at each position were examined, the M1−5 mutant (V176N) behaved like the wild-type enzyme. The M1−6 mutant (A177N), however,

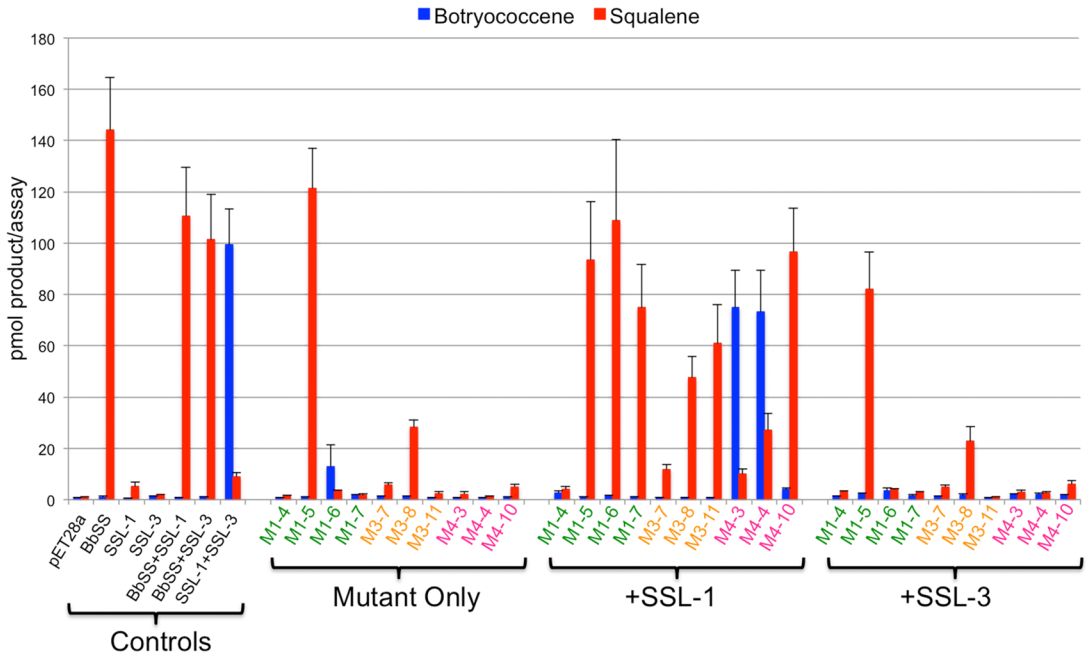

Figure 2. *In vitro* activity screens for BbSS and SSL-3 mutant enzymes listed in Table 1. Crude extracts of bacterially expressed enzymes were used as described in Figure S1 of the Supporting Information to assay a given enzyme's ability to perform the first or second reaction step of squalene and botryococcene biosynthesis or both.

dx.doi.org/10.1021/bi501264s | *Biochemistry* 2014, 53, 7570−7581

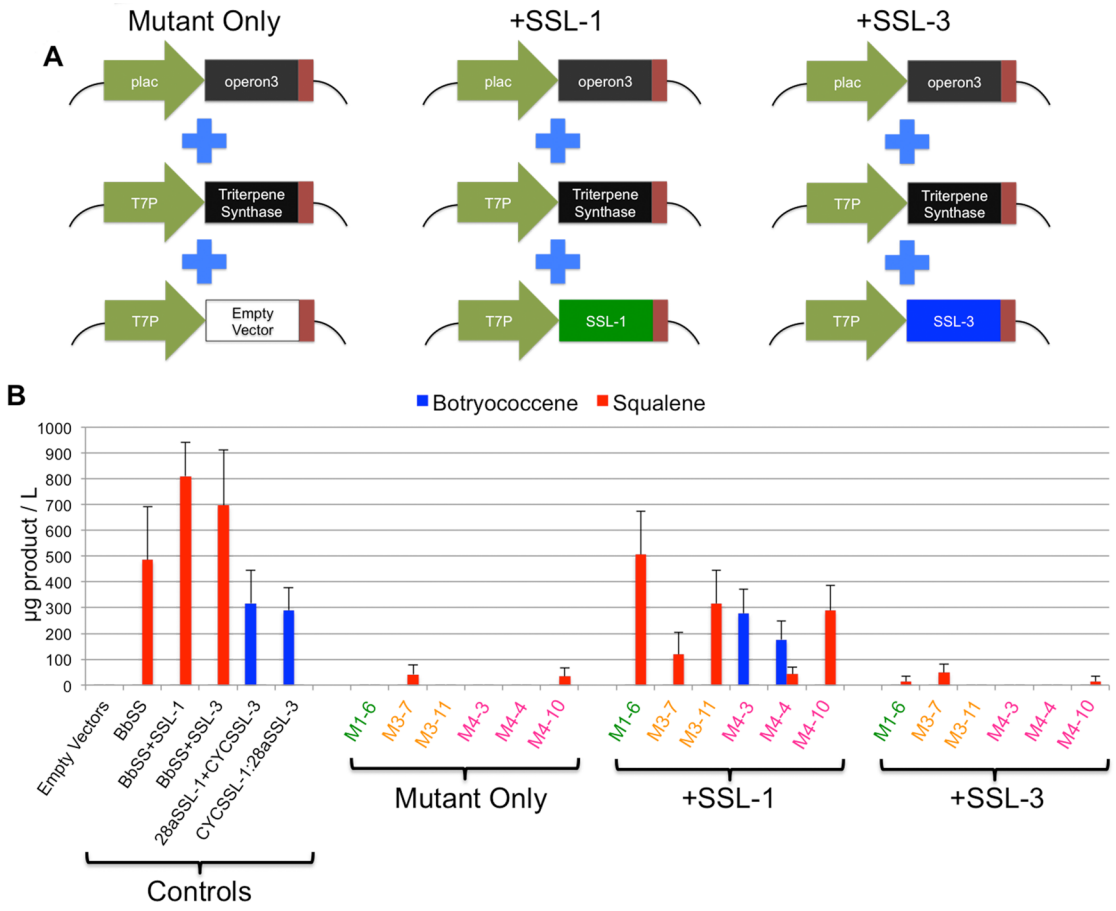

Figure 3. *In vivo* chemical profiling of BbSS and SSL-3 wild-type and mutant genes expressed in *E. coli* BL21(DE3) harboring pSB1:operon3. (A) Depiction of the general scheme used to analyze the mutant enzymes *in vivo* for their ability to catalyze the first or second reaction step of squalene or botryococcene biosynthesis or both. (B) Mutant genes were expressed in *E. coli* followed by chemical profiling of the cultures by GC−FID to quantify the levels of accumulation of squalene and botryococcene. Data shown are representative of three independent replicates (n = 3).

recapitulated the phenotype of the M1−7 double mutant. The M1−6 mutant retained the ability to convert PSPP to squalene but lost the ability to use FPP as a substrate. The M1 mutant series analyses thus suggested that position 177 was important for the first reaction step, the catalysis of FPP to PSPP, but not the second reaction step, and that position 176 was not critical for either reaction step.

Botryococcene was not observed in any of the assays with the M1 mutants, suggesting that residues in other domains might be more important for the PSPP to triterpene conversion specificity. Like the invariance of the amino acids at positions 176 and 177 in all squalene synthases, glutamine 213 in domain III is also completely conserved in squalene synthases across all kingdoms of life (Figure 1B). In SSL-3, which catalyzes PSPP to botryococcene, the position that corresponds to 213 is occupied by glycine. Hence, the glutamine at position 213 in the BbSS background was mutated to glycine (M3−7) and asparagine (M3−8) and evaluated for their catalytic specificities (Figure 2). Both of these mutants lost a significant proportion of their catalytic ability to convert FPP to squalene or any other hydrocarbon products. However, M3−8, which harbors the conservative substitution of asparagine for glutamine, retained approximately 20% of the wild-type BbSS enzyme activity. Both mutants also demonstrated an ability to accept PSPP as a substrate, albeit the activity levels were only 10 and 35% of that of the wild-type activity for M3−7 and M3−8, respectively. On the basis of the logic of Greenhagen et al. concerning the need for reciprocal, topological changes across the active site to accommodate the spatial needs for reaction intermediates to interconvert catalytic specificities among related terpene synthases,[33] the BbSS A177N/Q213G double mutant (M3−11) was created and evaluated. It too behaved much like the single mutants, having lost the first reaction step but retained a greater level of the second reaction step for the conversion of PSPP to squalene.

Contrary to our expectations, mutating the residues at positions 177 and 213 of BbSS to match the corresponding positions in SSL-3 did not change the reaction product specificity from squalene to botryococcene. Instead, these residues appeared to be more critical for the FPP to PSPP conversion. Thus, it was hypothesized that mutating the corresponding positions within the SSL-3 enzyme backbone would restore first-reaction step capability. When single mutants M4−3 and M4−4, corresponding to N171A and G207Q (positions synonymous to positions 177 and 213 in BbSS), respectively, were evaluated for activity, neither exhibited any hydrocarbon biosynthesis from FPP, but both biosynthesized botryococcene and small amounts of squalene upon incubation with SSL-1, a source of PSPP (Figure 2). Much to our surprise, however, the M4−10 double mutant that combined N171A and G207Q mutations into the SSL-3 backbone resulted in complete conversion of SSL-3 from an enzyme that used PSPP for botryococcene biosynthesis to one that used PSPP for squalene biosynthesis.

dx.doi.org/10.1021/bi501264s | *Biochemistry* 2014, 53, 7570−7581

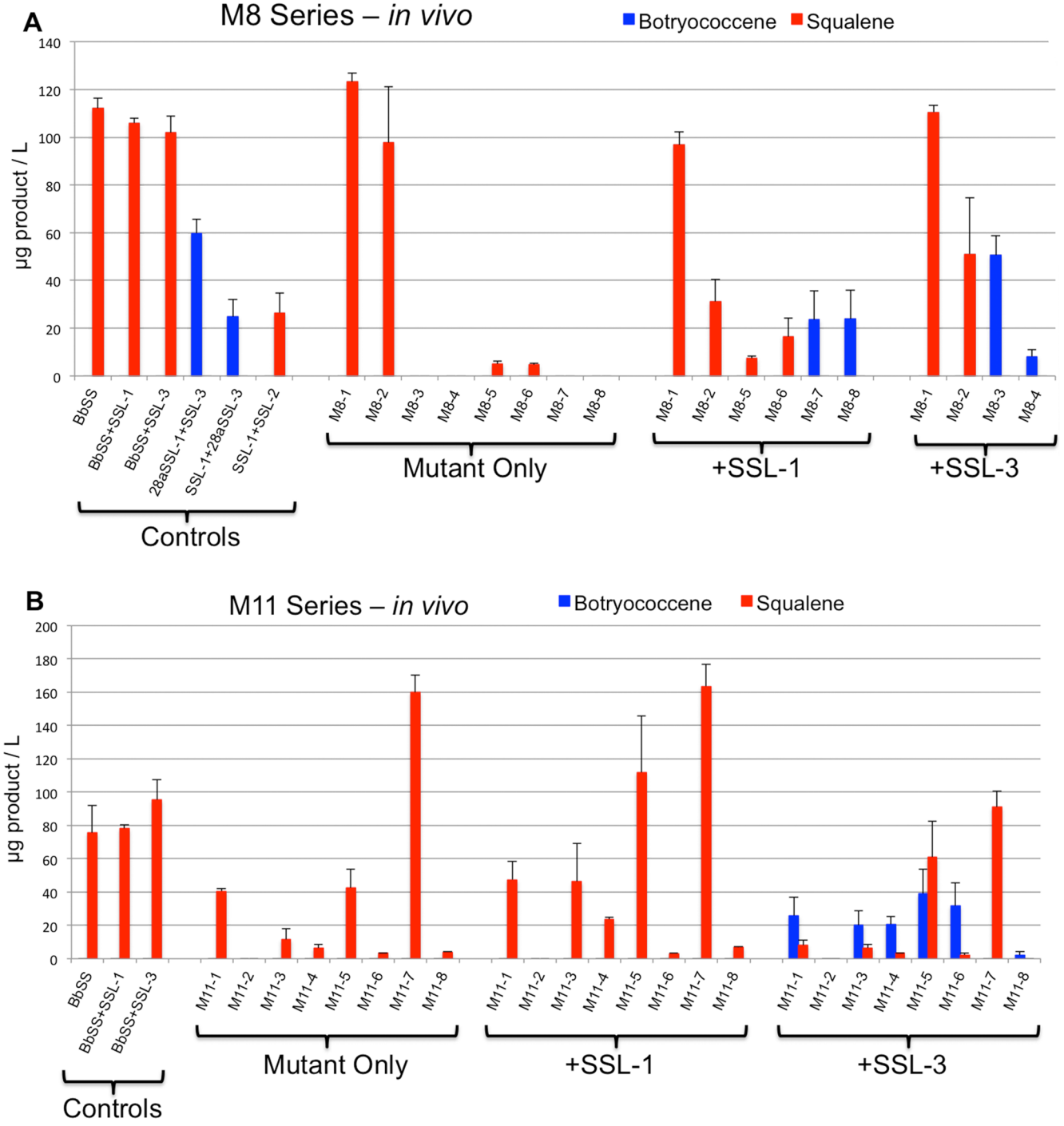

Figure 4. *In vivo* chemical profiling of the M8 and M11 mutant series for an assessment of highly conserved residues with respect to the first (+SSL-3), second (+SSL-1), and both (mutant only) reaction step capabilities. (A) The M8 mutant series (Table 2) focused on a highly conserved tyrosine residue in domain II that was mutated to Phe or Ala in BbSS, SSL-1, SSL-2, and SSL-3. (B) The M11 mutant series (Table 2) were directed at the conserved residues of the amino (M11−1 to M11−4) and carboxy (M11−5 to M11−8) RDXXED motifs, where the highlighted residues were individually substituted with Ala in the BbSS backbone. Mutant genes were expressed in *E. coli* followed by chemical profiling of the cultures by GC−FID to quantify the levels of accumulation of squalene and botryococcene. Data shown are representative of three independent replicates (n = 3).

GC−MS product profiling was conducted to verify the authenticity of the reaction products reported for the radiolabeled *in vitro* analyses (Figure S3A of the Supporting Information). Additionally, the dependence of the mutant triterpene synthases on NADPH for squalene and botryococcene biosynthesis was examined to ensure that utilization of this cofactor had not been altered in the mutant enzymes (Figure S3B of the Supporting Information). Minor amounts of enzyme activity were observed in reaction mixtures incubated without the addition of NADPH (Figure S3B of the Supporting Information), most likely due to reducing equivalents present in the bacterial lysates that were used as the enzyme sources.

***In Vivo* Confirmation of Mutant Phenotypes.** To verify the *in vitro* activity assays, an *in vivo* bacterial system was constructed in *E. coli* BL21(DE3). The approach mirrored efforts by others to produce terpenes in bacterial production

dx.doi.org/10.1021/bi501264s | *Biochemistry* 2014, 53, 7570−7581

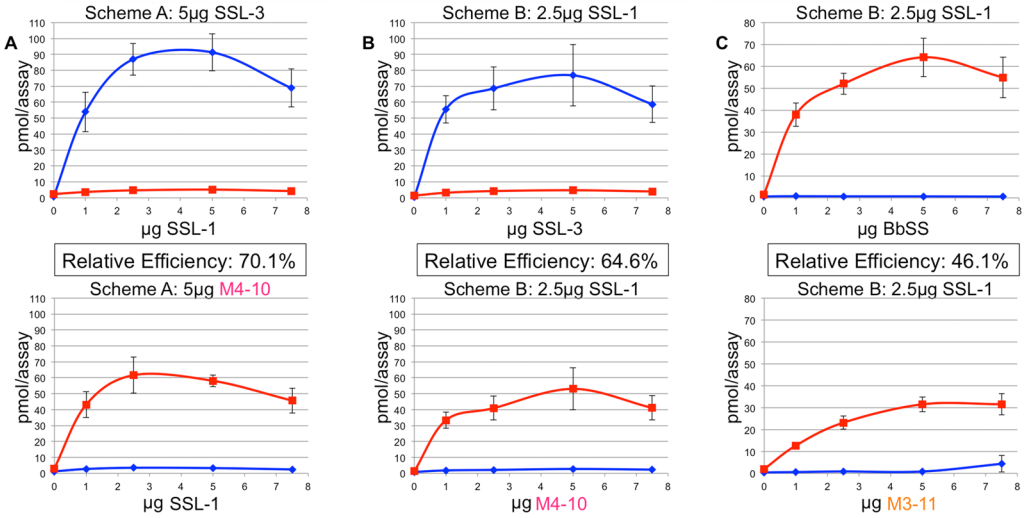

Figure 5. Relative catalytic efficiency assays for the M4−10 and M3−11 mutants. Panels A and B measure the biosynthetic activity of the M4−10 mutant for squalene upon co-incubation with SSL-1, a source enzyme for PSPP, in comparison to the wild-type SSL-3 enzyme's biosynthetic abilities for botryococcene. The M4−10 mutant was constructed by mutagenesis of the wild-type SSL-3 gene. Efficiency reflects the ability of the SSL-1 enzyme to produce saturating amounts of PSPP for the SSL-3 and M4−10 enzymes (A), as well as any physical interactions between the respective enzymes that might facilitate overall catalysis (B). Measurements of botryococcene and squalene biosynthetic activity with increasing amounts (0−7.5 μg) of SSL-1 crude lysate and a constant amount (5 μg) of SSL-3 (top) or M4−10 (bottom) crude lysate are reported in panel A, while the same measurements are reported for a constant amount (2.5 μg) of SSL-1 crude lysate and variable amounts (0−7.5 μg) of SSL-3 (top) or M4−10 (bottom) in panel B. In panel C, the relative efficiency of the M3−11 mutant enzyme (bottom) for squalene and botryococcene biosynthesis is compared to that of the wild-type BbSS enzyme (top), the scaffold upon which the M3−11 mutant was constructed. All assays contained 5 mM NADPH.

platforms and overexpressed key MEP biosynthetic genes encoding putative rate-limiting steps in the biosynthesis of the key five-carbon isoprenoid building blocks, IPP and DMAPP.[34,35] Plasmid vector pSB1:operon3 was constructed as a synthetic operon under the control of a lactose-inducible promoter (plac) and was comprised of the genes encoding 1-deoxy-D-xylulose-5-phosphate synthase (DXS), isopentenyl diphosphate isomerase (IDI), and farnesyl diphosphate synthase (FPS). Increased carbon flux was verified by co-expressing the wild-type BbSS gene individually with each of genes making up operon3, or the entire operon3, and measuring the accumulation of squalene in the bacterial cultures (Figure S4A of the Supporting Information). Squalene titers were on average 3 times higher when the complete operon3 was co-expressed with BbSS rather than any one gene of the operon (Figure S4B of the Supporting Information).

In vivo confirmation of the mutant enzyme phenotypes was conducted by expressing select mutants by themselves and in combination with either SSL-1 or SSL-3, much the same way *in vitro* assays were conducted to test for both reaction step capabilities (Figure 3A). Overall, the *in vivo* analyses confirmed the *in vitro* activity screens in which mutations at positions A177 and Q213 (M1−6, M3−7, and M3−11) abolish the first reaction step within BbSS without adversely affecting product specificity when supplied with a source of PSPP (i.e., SSL-1 co-expression) (Figure 3B). Also as seen in the *in vitro* assays, the single mutations N171A and G207Q (M4−3 and M4−4) within SSL-3 had a limited effect on botryococcene biosynthesis when provided a source of PSPP, but the N171A/G207Q double mutation appeared to be sufficient to convert product specificity from botryococcene to squalene (Figure 3B). Moreover, the products observed in the *in vivo* analyses were verified to be squalene and botryococcene by GC−MS analysis (Figure S3C of the Supporting Information).

Previous structure−function studies conducted using site-directed mutagenesis of the *Rattus norvegicus* squalene synthase (RnSS) suggested a couple of residues that were important for both reaction steps (Y171) or just the second reaction step (F288) based on the loss or reduction of catalytic activity as measured by *in vitro* assays.[4] Analogous mutants were constructed in the *B. braunii* squalene synthase and all three SSL enzymes in which the tyrosine corresponding to RnSS Y171 was mutated to phenyalanine and alanine (Table 2). Surprisingly, little if any contribution for this tyrosine residue to squalene (BbSS and SSL-2) or botryococcene (SSL-3) biosynthesis was observed, or to the first reaction step converting FPP to PSPP (SSL-1) (Figure 4A). In contrast, when charged residues putatively associated with coordinating a metal cofactor in the initial binding of the diphosphate groups associated with FPP and PSPP were mutated to the noncharged residue alanine in the BbSS enzyme (Table 2), overall activity was lost (M11−2) or dramatically reduced (M11−6) (Figure 4B). Additionally, these mutants also revealed the importance of these residues for the first and second reaction steps. For example, when mutants M11−1, −3, −4, −5, and −6 were co-expressed with SSL-3, significant amounts of botryococcene, derived from PSPP that must have been synthesized and released from the mutant BbSS enzyme to feed catalysis by SSL-3, accumulated in *E. coli*. Hence, residues R76, E82, D83, R219, and D220 are important not only for the initial binding of FPP in the active site (mutant only expression in *E. coli*) but also for the retention of PSPP in the active site and hence the second reaction step (comparison of both squalene and botryococcene levels in *E. coli* expressing only the mutant BbSS enzymes versus co-expression of both the mutant BbSS enzyme and SSL-3).

Assessment of the Catalytic Efficiency of the Mutant Enzymes. Determination of enzyme catalytic efficiencies

dx.doi.org/10.1021/bi501264s | *Biochemistry* 2014, 53, 7570−7581

typically involves purifying enzymes to homogeneity, followed by kinetic determinations of substrate affinity and turnover using Michaelis−Menten-like models. As noted above, PSPP is not commercially available, is technically challenging to prepare synthetically,[36,37] and is difficult to detect analytically. Further complicating this matter was the relatively quick loss of activity observed when mutant enzymes were assayed after purification (Figure S5 of the Supporting Information). Because of these complications, a strategy from Greenhagen et al. was exploited whereby varying enzyme amounts in a coupled assay could be used to glean information about a relative overall catalytic efficiency.[32] Using this approach, we estimated how efficiently M4−10 could catalyze squalene formation relative to botryococcene by SSL-3 via two different reaction schemes. Scheme A involved using increasing amounts of SSL-1 crude lysate (0, 1, 2.5, 5, and 7.5 μg) with the intention of providing increasing amounts of PSPP to achieve a "pseudokinetic" assessment of SSL-3 and M4−10; the second enzyme amount was held constant at 5 μg of crude lysate. The relative efficiency was calculated as a ratio of product formed by mutant enzyme to product formed by wild-type enzyme for each corresponding data point and expressed as a percentage. The overall relative efficiency was obtained by averaging the relative efficiencies across the entire data set. Scheme A assessment of M4−10 suggested a catalytic efficiency of 70.1% relative to SSL3 (Figure 5A). Scheme B was conducted like Scheme A with the exception that the amount of SSL-1 was held constant while the amount of SSL-3, M4−10, BbSS, or M3−11 was varied (0, 1, 2.5, 5, or 7.5 μg) for the second reaction step. This revealed an efficiency of 64.6% for M4−10 relative to SSL-3 (Figure 5B) and 46.1% for M3−11 relative to BbSS (Figure 5C).

DISCUSSION

Unraveling the structure−function relationships among the head-to-head coupling class of terpene synthases has been challenging, in part, because the distinct reaction steps associated with these enzymes were previously thought to be inseparable from those of enzymes like squalene synthase. Structure−function maps for squalene synthase were first suggested by Robinson et al. using protein sequence alignments with other known squalene and phytoene synthases.[15] These studies were then corroborated by crystallographic studies of HsSS and CrtM.[6,12−14] The 3D structures are all quite similar to one another, consisting of α-helical folds in which conserved domains I−IV line the active site pocket. Other notable features documented in crystallographic and site-directed mutagenesis work included the aspartate-rich (DXXED) motifs.[6,12] These motifs, along with arginine residues in their proximity, were proposed to coordinate the binding of magnesium−FPP/PSPP complexes in the active site pocket and facilitate the ionization events that lead to carbocation-mediated catalysis. Mutations within these domains were shown to severely limit or abolish catalytic activity.[4] Also identified were hydrophobic residues deep in the active site pocket, which compromised catalytic activity upon being mutated.[4] These residues presumably created particular topologies and weak surface charges that arose from π-orbitals of aromatic amino acid side chains that helped to coax reaction intermediates down specific catalytic cascades to their final reaction products.[38,39]

The work presented here has extended these observations by utilizing the squalene synthase-like enzymes to complement missing catalytic functions in the various mutants. For instance, mutation of the aspartate residues in either the amino- or carboxy-terminal DXXED motifs of the *B. braunii* squalene synthase essentially abolished the ability of the mutants to convert FPP to squalene, while mutations at either of the neighboring arginine residues only reduced activity by ∼50% (Figure 4B). In contrast, the glutamate residue within the amino-terminal DXXED motif was necessary for the conversion of FPP to squalene (M11−3), but the corresponding glutamate in the carboxy-terminal motif was not (M11−7) (Figure 4B). Co-expression of these mutants with either the SSL-1 or SSL-3 enzyme then provided an assessment for these enzymes' ability to perform either the first or second reaction step. Interestingly, many mutants, in either the amino- or carboxy-terminal DXXED motif, retained significant activity for the generation of PSPP, which was readily released and utilized by SSL-3 for botryococcene biosynthesis.

Our approach of trying to interconvert the reaction product specificities of squalene synthase and botryococcene synthase by reciprocal site-directed mutagenesis has also yielded new information about the amino acids controlling the 1′−1 and 1′−3 linkage specificity of the *B. braunii* triterpene synthases (Figure 2). Specifically, our results demonstrate that the amino acid residues at positions 171 and 207 within the SSL-3 enzyme can dictate product specificity. If N171 is changed to alanine and G207 is substituted with glutamine, changes that reflect conserved amino acids found in all squalene synthases at the corresponding positions, the SSL-3 double mutant switches to catalyzing squalene from PSPP instead of botryococcene from PSPP. Neither of the single mutants, N171A or G207Q, was sufficient for the complete conversion, which is analogous to the findings of Greenhagen et al. for the interconversion of sesquiterpene synthase enzyme activity,[33] the rationale being that the double mutants are spatial opposites of one another (Figure 6), creating a surface bulge on one side of the reaction pocket that is relieved by a size reduction on the other side of the pocket. Such mutants would thus constrain the confirmations available to a reaction intermediate as it cascades down a carbocation-mediated pathway (Scheme 1).

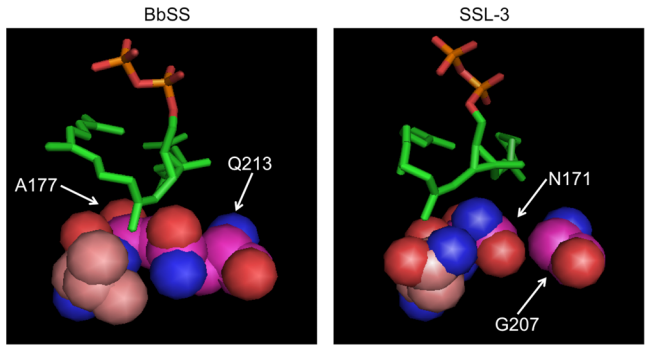

Figure 6. 3D models of BbSS and SSL-3 with PSPP docked into the active sites with only PSPP and the residues known to affect product specificity shown as spheres. The model depicts orientation of PSPP in relation to residues identified in this study that control product specificity in SSL-3. Residues shown with the carbon backbone as magenta spheres could be acting to orient PSPP in the active site such that C1′−C3 bond breakage and re-formation to C1′-1−2 is favored in BbSS while C1′−C2 bond breakage to yield a vinyl ethyl is favored in SSL-3.

If such an explanation were sufficient to account for the change in catalytic specificity of SSL-3, then one would have expected the reciprocal mutations in the *B. braunii* squalene

dx.doi.org/10.1021/bi501264s | *Biochemistry* 2014, 53, 7570−7581

synthase, A177N and Q213G, to yield a complete botryococcene synthase that catalyzed the conversion of FPP to PSPP and PSPP to botryococcene, but this was not observed. In fact, the single as well as double mutants tended to knock out the first reaction step of the BbSS enzyme, but the ability to utilize PSPP for the biosynthesis of squalene was retained. This contrasted with the analogous mutations within the SSL-3 enzyme, which had no effect on restoring the first-reaction step capability in these mutants but did control the product specificity of their second reaction step.

Our inability to identify complementary amino acid positions controlling the same catalytic and product specificity among the squalene and squalene-like enzymes may not be surprising in retrospect. The specific mutations we created were selected from the differences observed within the highly conserved regions of squalene synthases first identified by Robinson et al.[15] There are many other amino acid differences outside these "conserved" domains that undoubtedly contribute uniquely to the catalytic capacities of these enzymes. Hence, it might be more reasonable to expect mutations to be context-dependent, meaning that the mutations are dependent upon the enzyme background in which they are present.

The inability of the reciprocal double mutants to fully interconvert squalene synthase into a botryococcene synthase might also be related to the recent observations of Liu et al. and Furubayashi et al.[12,16] These investigators have described a nonconventional NADPH binding site in squalene synthases, which would play an essential role in presenting reducing equivalents from NADPH to the reactive intermediate undergoing a reductive rearrangement. Hence, the nonconserved residues making up the NADPH binding site and its surroundings might play a role in orchestrating the stereoelectronics for how reducing equivalents are fed into the active site pocket and thus influence reaction product outcomes.[21]

A final explanation of why the reciprocal mutations in squalene synthase behave differently than expected arises from the earlier observations of Lin et al. for a bacterial dehydrosqualene synthase.[14] On the basis of crystallographic determinations of analogues positioned in the CrtM enzyme, these authors suggested that formation of the PSPP intermediate was followed by its migration to another catalytic area, in effect repositioning the PSPP for the second reaction step. While a role of the DXXED motifs in these catalytic and migration events is certainly possible, other nonconserved residues spatially surrounding the DXXED motifs may be equally critical for the positioning of PSPP for the 1′−1 rearrangement found in squalene versus the 1′−3 rearrangement that occurs to yield botryococcene (Scheme 1). Our molecular modeling, which was based on sequence similarities and conserved amino acid domains, would be blind to such residues, and hence, their contribution to catalytic specificity would be overlooked.

Given the aim of mapping catalytic functions to specific features of triterpene synthases, we wonder if the rational design−mutagenesis approach described herein is actually efficient enough to unravel all the different ways by which the 1′−1 and 1′−3 linkages of triterpene synthases can be identified. Instead, we envision the need for a high-throughput screen that can select for desired mutants after a more exhaustive, iterative, and unbiased mutagenesis protocol.

■ ASSOCIATED CONTENT

Supporting Information

Figures and tables for the *in vitro* assay rationale, enzyme quality assessments, GC data, carbon flux analysis, conserved domain differences between SSL-1 and SSL-3, and cloning−mutagenesis primers. This material is available free of charge via the Internet at http://pubs.acs.org.

■ AUTHOR INFORMATION

Corresponding Author

*E-mail: chappell@uky.edu. Phone: (859) 218-0775.

Present Addresses

[§]T.D.N.: Horticultural Sciences, University of Florida, Gainesville, FL 32611.

[∥]S.E.N.: College of Pharmacy, Ferris State University, Big Rapids, MI 49307.

Funding

This work was supported, in part, by a grant from the National Science Foundation (CBET-0828817) and a research contract with Sapphire Energy, Inc. (San Diego, CA).

Notes

The authors declare the following competing financial interests: J.C. has a financial interest in TerGen Biotechnology, Inc.

■ ACKNOWLEDGMENTS

We are indebted to Scott Kinison for technical support throughout the course of this work.

■ ABBREVIATIONS

FPP, farnesyl diphosphate; PSPP, presqualene diphosphate; BbSS, *B. braunii* squalene synthase; SSL-1, squalene synthase-like 1; SSL-2, squalene synthase-like 2; SSL-3, squalene synthase-like 3; HsSS, *H. sapiens* squalene synthase; CrtM, *St. aureus* dehydrosqualene synthase; RnSS, *R. norvegicus* squalene synthase; AtSS, *Arabidopsis thaliana* squalene synthase; MEP, methylerythritol phosphate; IPP, isopentenyl diphosphate; DMAPP, dimethylallyl diphosphate; DXS, 1-deoxy-D-xylulose-5-phosphate synthase; IDI, isopentenyl diphosphate isomerase; FPS, farnesyl diphosphate synthase; plac, lactose promoter; NADPH, nicotinamide adenine dinucleotide phosphate.

■ REFERENCES

(1) Hannich, J. T., Umebayashi, K., and Riezman, H. (2011) Distribution and functions of sterols and sphingolipids. *Cold Spring Harbor Perspect. Biol. 3*, DOI: 10.1101/cshperspect.a004762.

(2) Siedenburg, G., and Jendrossek, D. (2011) Squalene-Hopene Cyclases. *Appl. Environ. Microbiol. 77*, 3905−3915.

(3) Blagg, B. S. J., Jarstfer, M. B., Rogers, D. H., and Poulter, C. D. (2002) Recombinant squalene synthase. A mechanism for the rearrangement of presqualene diphosphate to squalene. *J. Am. Chem. Soc. 124*, 8846−8853.

(4) Gu, P., Ishii, Y., Spencer, T. A., and Shechter, I. (1998) Function-structure studies and identification of three enzyme domains involved in the catalytic activity in rat hepatic squalene synthase. *J. Biol. Chem. 273*, 12515−12525.

(5) Jarstfer, M. B., Blagg, B. S. J., Rogers, D. H., and Poulter, C. D. (1996) Biosynthesis of Squalene. Evidence for a Tertiary Cyclopropylcarbinyl Cationic Intermediate in the Rearrangement of Presqualene Diphosphate to Squalene. *J. Am. Chem. Soc. 118*, 13089−13090.

(6) Pandit, J., Danley, D. E., Schulte, G. K., Mazzalupo, S., Pauly, T. A., Hayward, C. M., Hamanaka, E. S., Thompson, J. F., and Harwood,

H. J. (2000) Crystal structure of human squalene synthase. A key enzyme in cholesterol biosynthesis. *J. Biol. Chem. 275*, 30610−30617.
(7) Rilling, H. C. (1966) A New Intermediate in the Biosynthesis of Squalene. *J. Biol. Chem. 241*, 3233−3236.
(8) Epstein, W. W., and Rilling, H. C. (1970) Studies on the Mechanism of Squalene Biosynthesis. *J. Biol. Chem. 245*, 4597−4605.
(9) Radisky, E. S., and Poulter, C. D. (2000) Squalene synthase: Steady-state, pre-steady-state, and isotope-trapping studies. *Biochemistry 39*, 1748−1760.
(10) Jarstfer, M. B., Zhang, D.-L., and Poulter, C. D. (2002) Recombinant squalene synthase. Synthesis of non-head-to-tail isoprenoids in the absence of NADPH. *J. Am. Chem. Soc. 124*, 8834−8845.
(11) Pan, J.-J., Bugni, T. S., and Poulter, C. D. (2009) Recombinant Squalene Synthase. Synthesis of Cyclopentyl Non-Head to Tail Triterpenes. *J. Org. Chem. 74*, 7562−7565.
(12) Liu, C.-I., Jeng, W.-Y., Chang, W.-J., Shih, M.-F., Ko, T.-P., and Wang, A. H.-J. (2014) Structural insights into the catalytic mechanism of human squalene synthase. *Acta Crystallogr. D70*, 231−241.
(13) Liu, C.-I., Jeng, W.-Y., Chang, W.-J., Ko, T.-P., and Wang, A. H.-J. (2012) Binding modes of zaragozic acid A to human squalene synthase and staphylococcal dehydrosqualene synthase. *J. Biol. Chem. 287*, 18750−18757.
(14) Lin, F.-Y., Liu, C.-I., Liu, Y.-L., Zhang, Y., Wang, K., Jeng, W.-Y., Ko, T.-P., Cao, R., Wang, A. H.-J., and Oldfield, E. (2010) Mechanism of action and inhibition of dehydrosqualene synthase. *Proc. Natl. Acad. Sci. U.S.A. 107*, 21337−21342.
(15) Robinson, G. W., Tsay, Y. H., Kienzle, B. K., Smith-Monroy, C. A., and Bishop, R. W. (1993) Conservation between human and fungal squalene synthetases: Similarities in structure, function, and regulation. *Mol. Cell. Biol. 13*, 2706−2717.
(16) Furubayashi, M., Li, L., Katabami, A., Saito, K., and Umeno, D. (2014) Directed evolution of squalene synthase for dehydrosqualene biosynthesis. *FEBS Lett. 588*, 3375−3381.
(17) Metzger, P., and Largeau, C. (2005) *Botryococcus braunii*: A rich source for hydrocarbons and related ether lipids. *Appl. Microbiol. Biotechnol. 66*, 486−496.
(18) Eroglu, E., Okada, S., and Melis, A. (2011) Hydrocarbon productivities in different *Botryococcus* strains: Comparative methods in product quantification. *J. Appl. Phycol. 23*, 763−775.
(19) Poulter, C. D., Marsh, L. L., Hughes, J. M., Argyle, J. C., Satterwhite, D. M., Goodfellow, R. J., and Moesinger, S. G. (1977) Model Studies of Biosynthesis of Non-Head-to-Tail Terpenes. Rearrangements of the Chrysanthemyl System. *J. Am. Chem. Soc. 99*, 3816−3823.
(20) Huang, Z., and Poulter, C. D. (1989) Stereochemical studies of botryococcene biosynthesis: Analogies between 1′-1 and 1′-3 condensations in the isoprenoid pathway. *J. Am. Chem. Soc. 111*, 2713−2715.
(21) Poulter, D. C. (1990) Biosynthesis of Non-Head-to-Tail Terpenes. Formation of 1′-1 and 1′-3 Linkages. *Acc. Chem. Res. 23*, 70−77.
(22) Niehaus, T. D., Okada, S., Devarenne, T. P., Watt, D. S., Sviripa, V., and Chappell, J. (2011) Identification of unique mechanisms for triterpene biosynthesis in *Botryococcus braunii*. *Proc. Natl. Acad. Sci. U.S.A. 108*, 12260−12265.
(23) Okada, S., Devarenne, T. P., Murakami, M., Abe, H., and Chappell, J. (2004) Characterization of botryococcene synthase enzyme activity, a squalene synthase-like activity from the green microalga *Botryococcus braunii*, Race B. *Arch. Biochem. Biophys. 422*, 110−118.
(24) Sali, A., Potterton, L., Yuan, F., van Vlijmen, H., and Karplus, M. (1995) Evaluation of comparative protein modeling by MODELLER. *Proteins 23*, 318−326.
(25) Jones, G., Willett, P., and Glen, R. C. (1995) Molecular recognition of receptor sites using a genetic algorithm with a description of desolvation. *J. Mol. Biol. 245*, 43−53.
(26) Schüttelkopf, A. W., and van Aalten, D. M. F. (2004) PRODRG: A tool for high-throughput crystallography of protein-ligand complexes. *Acta Crystallogr. D60*, 1355−1363.
(27) Okada, S., Devarenne, T. P., and Chappell, J. (2000) Molecular characterization of squalene synthase from the green microalga *Botryococcus braunii*, race B. *Arch. Biochem. Biophys. 373*, 307−317.
(28) Higuchi, R., Krummel, B., and Saiki, R. K. (1988) A general method of in vitro preparation and specific mutagenesis of DNA fragments: Study of protein and DNA interactions. *Nucleic Acids Res. 16*, 7351−7367.
(29) Kovach, M. E., Elzer, P. H., Hill, D. S., Robertson, G. T., Farris, M. A., Roop, R. M., and Peterson, K. M. (1995) Four new derivatives of the broad-host-range cloning vector pBBR1MCS, carrying different antibiotic-resistance cassettes. *Gene 166*, 175−176.
(30) Ind, A. C., Porter, S. L., Brown, M. T., Byles, E. D., de Beyer, J. A., Godfrey, S. A., and Armitage, J. P. (2009) Inducible-expression plasmid for *Rhodobacter sphaeroides* and *Paracoccus denitrificans*. *Appl. Environ. Microbiol. 75*, 6613−6615.
(31) Shine, J., and Dalgarno, L. (1975) Determinant of cistron specificity in bacterial ribosomes. *Nature 254*, 34−38.
(32) Greenhagen, B. T., Griggs, P., Takahashi, S., Ralston, L., and Chappell, J. (2003) Probing sesquiterpene hydroxylase activities in a coupled assay with terpene synthases. *Arch. Biochem. Biophys. 409*, 385−394.
(33) Greenhagen, B. T., O'Maille, P. E., Noel, J. P., and Chappell, J. (2006) Identifying and manipulating structural determinates linking catalytic specificities in terpene synthases. *Proc. Natl. Acad. Sci. U.S.A. 103*, 9826−9831.
(34) Lv, X., Xu, H., and Yu, H. (2013) Significantly enhanced production of isoprene by ordered coexpression of genes dxs, dxr, and idi in *Escherichia coli*. *Appl. Microbiol. Biotechnol. 97*, 2357−2365.
(35) Kim, S., and Keasling, J. D. (2001) Metabolic Engineering of the Nonmevalonate Isopentenyl Diphosphate Synthesis Pathway in *Escherichia coli* Enhances Lycopene Production. *Biotechnol. Bioeng. 72*, 408−415.
(36) Rogers, D. H., Yi, E. C., and Poulter, C. D. (1995) Enantioselective Synthesis of (+)-Presqualene Diphosphate. *J. Org. Chem. 60*, 941−945.
(37) Coates, R. M., and Robinson, W. H. (1971) Stereoselective Total Synthesis of (±)-Presqualene Alcohol. *J. Am. Chem. Soc. 93*, 1785−1786.
(38) Johnson, W. S. (1991) Fifty Years of Research. A Tribute to My Co-workers. *Tetrahedron 47*, xi−l.
(39) Dougherty, D. A. (1996) Cation-π Interactions in Chemistry and Biology: A New View of Benzene, Phe, Tyr, Trip. *Science 271*, 163−168.
(40) Thulasiram, H. V., Erickson, H. K., and Poulter, C. D. (2008) A common mechanism for branching, cyclopropanation, and cyclobutanation reactions in the isoprenoid biosynthetic pathway. *J. Am. Chem. Soc. 130*, 1966−1971.